Available online at www.sciencedirect.com

ScienceDirect

Geochimica et Cosmochimica Acta 148 (2015) 269–283

Geochimica et Cosmochimica Acta

www.elsevier.com/locate/gca

Biogeochemical cycling of cadmium isotopes along a high-resolution section through the North Atlantic Ocean

Tim M. Conway *, Seth G. John

Department of Earth and Ocean Sciences, University of South Carolina, Columbia, SC 29208, USA

Received 31 May 2014; accepted in revised form 22 September 2014; available online 22 October 2014

Abstract

Cadmium (Cd) is a bioactive trace element in the oceans, with a nutrient-like distribution that closely matches dissolved phosphate. Seawater-dissolved stable Cd isotope ratios (δ^{114}Cd) are a relatively new parameter, which show much promise for furthering our understanding of the biogeochemical cycling of Cd in the oceans. Here we present a high-resolution paired section of dissolved Cd concentrations and dissolved δ^{114}Cd from 21 open-ocean stations along the US GEOTRACES GA03 transect through the North Atlantic Ocean. Dissolved Cd concentrations along the section are strongly influenced by water-mass distribution and the cycling of Cd. The highest dissolved Cd concentrations (400–540 pmol kg^{-1}) are associated with Antarctic-sourced water masses, whilst biological uptake in the surface ocean results in a strong vertical gradient in dissolved Cd towards the surface, reaching as low as 0.03 pmol kg^{-1} in western surface waters. Dissolved δ^{114}Cd is also characterized by a vertical gradient from ~+0.2‰ in the deep ocean to +2‰ to +5‰ in the Cd-depleted surface ocean (relative to NIST SRM 3108). This variability in δ^{114}Cd can be ascribed to mixing of Antarctic and North Atlantic water masses, together with fractionation due to *in situ* biological uptake of light Cd in the very surface ocean. Subtle deviations from this overall pattern of dissolved Cd concentration and dissolved δ^{114}Cd are observed within low-oxygen waters off North Africa, where a dissolved Cd deficit relative to phosphate is associated with higher dissolved δ^{114}Cd values. Together with elevated particulate Cd and Ba, this suggests that Cd sulfide precipitation is occurring within the water column of the North Atlantic, constituting a potentially important sink for isotopically light Cd. Additionally, the first measurements of dissolved δ^{114}Cd within a hydrothermal plume at the Mid-Atlantic Ridge show that Cd is scavenged from the dissolved phase, leaving the remnant dissolved Cd isotopically heavier. Constraining the significance of these marine sinks for dissolved Cd is important, not only for our understanding of the marine biogeochemical cycling of Cd in the modern oceans, but also for the successful application of the microfossil Cd/Ca proxy and the development of δ^{114}Cd as a tracer for past-ocean biogeochemical cycling.

1. INTRODUCTION

Cadmium (Cd) is a biologically active trace element in the oceans, where it may possibly be a micronutrient under some conditions, replacing zinc or cobalt in enzymes such as carbonic anhydrase within marine phytoplankton (Price and Morel, 1990; Lane and Morel, 2000; Lane et al., 2005), or it may be a toxin (e.g., Sunda and Huntsman, 1996; Horner et al., 2013). Cd has a spatial marine distribution which closely matches the major nutrients nitrate and phosphate (Boyle et al., 1976; Bruland, 1980), driven principally by uptake into biological material at the surface, regeneration of this organic material with depth and physical circulation of the oceans. Consequently, dissolved Cd concentrations range from less than 1 pmol kg^{-1} in depleted surface waters to as high as 1000 pmol kg^{-1}

* Corresponding author. Present address: Institute for Geochemistry and Petrology, Department of Earth Sciences, ETH Zürich, Zürich 8092, Switzerland. Tel.: +41 44 632 4797.

E-mail address: conway.tm@gmail.com (T.M. Conway).

http://dx.doi.org/10.1016/j.gca.2014.09.032
0016-7037/

within the deep Pacific Ocean, where older water masses have accumulated regenerated Cd (e.g., Biller and Bruland, 2012). The close relationship between dissolved Cd and phosphate (PO_4^{3-}) concentrations observed throughout the modern oceans has facilitated the use of Cd/Ca ratios in microfossils as a paleoproxy for both marine nutrient utilization and water mass distributions in the past (e.g., Boyle, 1988; Elderfield and Rickaby, 2000). However, successful application of this proxy relies on an understanding of how biogeochemical processes influence the global Cd/PO_4^{3-} ratio and the differing Cd/PO_4^{3-} signatures of different water masses. These processes include preferential biological uptake of Cd over PO_4^{3-} in Antarctic surface waters (e.g., Gault-Ringold et al., 2012; Baars et al., 2014), or Cd sulfide precipitation within sediments or the water column itself (Rosenthal et al., 1995; van Geen et al., 1995; Janssen et al., 2014).

Seawater dissolved stable cadmium isotope ratios (denoted here by $\delta^{114}Cd$) are a recently-developed oceanographic tracer (Lacan et al., 2006; Ripperger and Rehkämper, 2007) that have now been utilized by a number of studies to draw insights into the biogeochemical processes influencing the marine distribution of Cd (Ripperger et al., 2007; Ho et al., 2009; Abouchami et al., 2011, 2014; Gault-Ringold et al., 2012; Yang et al., 2012; Xue et al., 2013). Globally, the deep oceans >1000 m are characterized by a homogenous $\delta^{114}Cd$ value that is close to +0.3‰ (Ripperger et al., 2007; Xue et al., 2012, 2013; Yang et al., 2012; Conway et al., 2013; Abouchami et al., 2014). Biological uptake of Cd into phytoplankton, with a biological preference for assimilation of lighter isotopes leads to a monotonic increase towards heavier values in the surface ocean, where dissolved $\delta^{114}Cd$ may exceed +2‰ as dissolved Cd concentrations become increasingly depleted (Lacan et al., 2006; Ripperger et al., 2007; Horner et al., 2013; John and Conway, 2014). Most recently, marine $\delta^{114}Cd$ studies have focused on investigating the biological cycling of Cd in the Southern Ocean, where both water-mass mixing and biological cycling influence $\delta^{114}Cd$ (Abouchami et al., 2011, 2014; Gault-Ringold et al., 2012; Xue et al., 2013), or on the global sinks of Cd from the oceans (Janssen et al., 2014). Such studies highlight two areas where $\delta^{114}Cd$ measurements may be influential in providing constraints on both the modern marine Cd cycle and the application of Cd/Ca or $\delta^{114}Cd$ as paleo-proxies.

Seawater dissolved $\delta^{114}Cd$ measurements show the isotopic signature of the deep ocean <1000 m in the North Pacific (+0.2‰ to +0.3‰), the Southern Ocean (+0.24‰ to +0.25‰), and the South China Sea (+0.24‰) to be homogenous. (Ripperger et al., 2007; Xue et al., 2012, 2013; Yang et al., 2012; Conway et al., 2013; Abouchami et al., 2014). By contrast, the deep North Atlantic is slightly heavier (+0.23‰ to +0.5‰; Boyle et al., 2012; Xue et al., 2012; Conway et al., 2013). Worldwide, the deep ocean is isotopically heavier than the near-crustal signature of potential inputs to the ocean (~+0.1‰), suggestive of a net isotopically-lighter sink of Cd from the oceans (data from Lambelet et al., 2013 and Schmitt et al., 2009 converted to NIST-3108 in Rehkämper et al., 2012). Based partly on a subset of data presented here, Cd sulfide precipitation within low-oxygen waters of the global oceans has been recently proposed as an important isotopically light sink for Cd from the oceans (Janssen et al., 2014). If confirmed, a marine sulfide sink for Cd may account for the isotopically heavy global deep ocean and may have been influential in setting both the global deep ocean $\delta^{114}Cd$ signature and the Cd/PO_4^{3-} of the oceans in the past.

Here, we present the first high-resolution paired ocean section of dissolved Cd concentration and dissolved Cd stable isotope ratio ($\delta^{114}Cd$) along a transect in the North Atlantic Ocean. We present data from 574 samples from 21 stations from the US GEOTRACES GA03 North Atlantic Transect, which sailed from Lisbon to Woods Hole, via Mauritania and the Mid-Atlantic Ridge. This large dataset allows us to investigate the marine cycling of Cd and $\delta^{114}Cd$ at the basin scale, and, in particular, to focus on Cd removal processes such as Cd sulfide formation in low-oxygen waters of the North Atlantic and the influence of hydrothermal vents on the dissolved Cd reservoir. Complementing the dissolved Cd data, we also present particulate Ba and Cd concentration from 12 stations along the section, allowing us to further explore the partitioning of Cd between the particulate and dissolved phases under variable oceanographic conditions. The data presented in this study are deposited with the Biological and Chemical Oceanography Data Management Office (BCO-DMO) and are also available as Supplementary Data. Continuous temperature, salinity and oxygen data for the GA03 Section are available from BCO-DMO (http://www.bco-dmo.org/project/2066).

2. METHODS

2.1. North Atlantic sampling

North Atlantic seawater and particulate samples were collected during the US GEOTRACES GA03 North Atlantic transect cruises, consisting of two cruise legs on board the R/V Knorr in October–November 2010 (USGT10) and November–December 2011 (USGT11). Twenty-one open-ocean stations (25–37 point depth profiles) were sampled across both cruises for dissolved Cd concentration and $\delta^{114}Cd$; 8 stations on USGT10 (USGT10-1, 3, 5, 7, 9, 10, 11 and 12) and 13 on USGT11 (USGT11-1, 2, 3, 6, 8, 10, 12, 14, 16, 18, 20, 22 and 24), with occupation of a crossover station on both cruises (USGT10-12, USGT11-24) close to Cape Verde (17.4°N, 24.5°W). Station locations are shown in Fig. 1, overlain on minimum water-column dissolved oxygen concentration. Seawater was collected by the GEOTRACES sampling team, either with GO-FLO bottles on the GEOTRACES rosette (>2 m depth) or with surface towfish (~2 m) and then filtered with 0.2 μm Pall Acropak-200 Supor cartridges (Cutter and Bruland, 2012). Filtered seawater samples were later acidified to pH ~2 by addition of 1 mL 12 mol L^{-1} Aristar Ultra™ hydrochloric acid at the University of South Carolina and then left for several months before processing and analysis for dissolved Cd and $\delta^{114}Cd$.

Suspended particle samples (0.8–51 μm and >51 μm) were collected at 22 of the stations (16 point depth

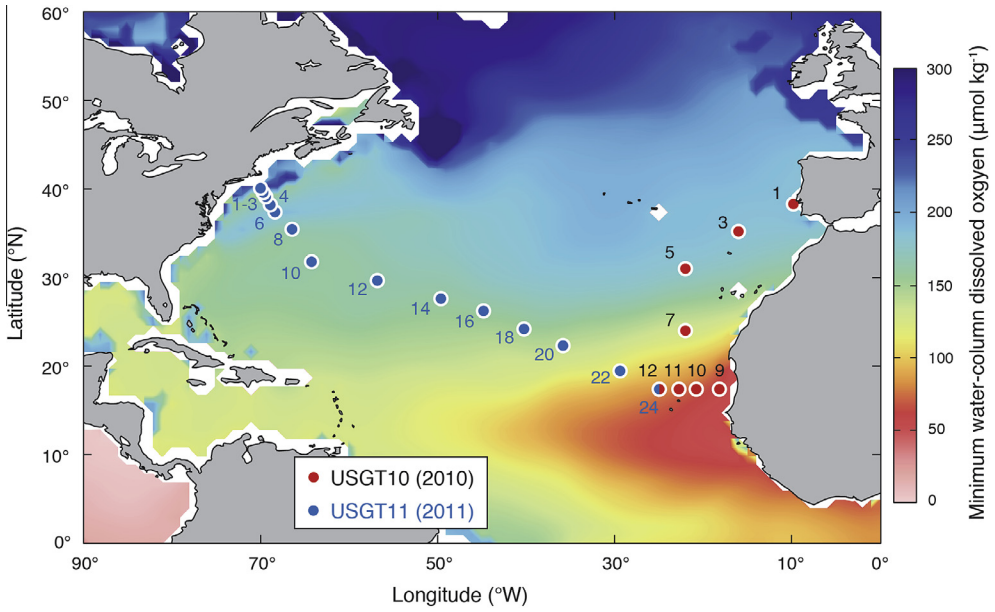

Fig. 1. Cruise track of the US GEOTRACES GA03 North Atlantic Transect. Stations sampled during this study on both the 2010 (USGT10) and 2011 (USGT11) cruise legs are shown, overlain on minimum water column dissolved oxygen concentration from the 2009 World Ocean Atlas database, highlighting the pronounced oxygen minimum region close to North West Africa. (For interpretation of the references to color in this figure legend, the reader is referred to the web version of this article.)

profiles) occupied during the USGT10 and USGT11 cruises, using in-situ battery powered McLane pumps as described by Ohnemus and Lam (2014). Of these 22 stations, 12 (USGT10-1, 9, 10, 11, 12 and USGT11-4, 8, 10, 12, 14, 16, 20) were sampled in this study for particulate Cd, barium (Ba) and phosphate (P) concentration. Suspended phase (0.8–51 µm) samples were supplied by Lam and Ohnemus as portions of the 142 mm diameter 0.8 µm polyethersulfone filters used for shipboard collection.

2.2. Sample processing and analysis

All samples were processed in the Marine Trace Element Laboratories at the University of South Carolina in flow benches under ULPA filtration. All water used was ultrapure (>18.2 MΩ) and all acids and reagents were Aristar Ultra™ obtained from VWR international (seawater samples) or from in-house quartz and Teflon distillation procedures (particulate samples). All plasticware was rigorously acid-cleaned prior to use, following Conway et al. (2013). All ICPMS analyses were carried out at the Center for Elemental Mass Spectrometry at the University of South Carolina.

2.2.1. Seawater dissolved Cd and $\delta^{114}Cd$

Seawater samples were processed and analyzed for dissolved Cd and $\delta^{114}Cd$ using a double-spike technique, following previously published methods (Conway et al., 2013). Briefly, 1 L samples were spiked prior to processing with a ^{110}Cd–^{111}Cd double spike in an approx. 1:4 sample to spike ratio, and then Cd was quantitatively extracted onto Nobias PA-1 resin (Hitachi) using a batch-extraction technique in seawater pH-adjusted to pH ~6.2. Cd was then effectively separated from interferences such as Mo, Sn and major salts using AGMP-1 anion exchange resin (Conway et al., 2013). Cd from samples was dissolved in 0.1 mol L^{-1} HNO_3 for analysis by Thermo Neptune MC-ICPMS in low-resolution, with Pt Jet and Al 'x-type' skimmer cones. Samples were introduced using a borosilicate glass nebulizer and ESI Apex-Q desolvation system without desolvation membrane. Each seawater sample was analyzed twice by MC-ICPMS and an average value calculated for Cd concentration and $\delta^{114}Cd$, with the exception of very low concentration Cd samples, where there was only sufficient Cd for a single ICPMS analysis.

Dissolved Cd concentrations were calculated using isotope-dilution from addition of double spike and the original weight of each seawater sample. We assign 2% error to all Cd concentrations to account for pipetting and weighing error. The procedural blank was previously calculated to be $\leqslant$0.04 pmol kg^{-1} by Conway et al. (2013), and this assessment is supported by dissolved Cd concentrations as low as 0.03 pmol kg^{-1} in this study. Dissolved $\delta^{114}Cd$ was calculated using the double spike data reduction scheme described in Conway et al. (2013), following the iterative approach of Siebert et al. (2001). Each group of 6 samples was analyzed by MC-ICPMS bracketed by two analyses of a NIST SRM 3108 Cd double-spike standard solution, with concentration and sample:spike ratio both designed to closely match samples. NIST SRM 3108 Cd has recently been the focus of a community-wide intercalibration effort (Abouchami et al., 2013), and we therefore express all Cd isotope ratios in delta notation, relative to the mean $\delta^{114}Cd$ of these two NIST SRM 3108 standards:

$$\delta^{114}\mathrm{Cd}\ (‰) = \left[\frac{\left(\frac{^{114}\mathrm{Cd}}{^{110}\mathrm{Cd}}\right)_{\mathrm{sample}}}{\left(\frac{^{114}\mathrm{Cd}}{^{110}\mathrm{Cd}}\right)_{\mathrm{NIST\ SRM\ 3108}}} - 1\right] * 1000$$

Although some studies report Cd stable isotope ratios in ε notation, we instead use δ notation (this study; Conway et al., 2013; John and Conway, 2014; Janssen et al., 2014) so that data is more easily comparable with the other marine bioactive trace elements (δ^{56}Fe, δ^{66}Zn, δ^{65}Cu, δ^{60}Ni), which have similar magnitudes of δ variability in seawater.

We express 2σ uncertainty on δ^{114}Cd as the combined internal standard error of samples and bracketing NIST SRM 3108 standards as calculated previously (Conway et al., 2013), based on the observation that uncertainty with MC-ICPMS double spike technique is dominated by internal error (John, 2012). 2σ uncertainty depends on Cd concentration, with typical values of 0.04–0.06‰ for ⩾100 pmol kg^{-1}, 0.06–0.2‰ for 10–100 pmol kg^{-1} and 0.2–1.5‰ for samples <10 pmol kg^{-1} (see Supplementary Data).

Previously published measurements of dissolved Cd concentration in SAFe S and D seawater standards using this technique demonstrated excellent agreement with the most recent (May 2013) SAFe consensus values (Conway et al., 2013). We also find good agreement between independent measurement of dissolved Cd concentration using different techniques at 5 stations across the GA03 section analyzed at USC (this study) and UC Santa Cruz (Middag and Bruland, data in Schlitzer, 2014) as well as between dissolved Cd concentrations published for the GEOTRACES IC1 cruise by the authors (Conway et al., 2013) and by several other laboratories (Boyle et al., 2012). External accuracy of our δ^{114}Cd measurements was shown by good agreement with the multiple-lab consensus separation of BAM and Münster Cd international isotope standards from NIST SRM 3108 (Abouchami et al., 2013; Conway et al., 2013). We also showed good agreement between two laboratories for measurements of dissolved δ^{114}Cd of +0.3‰ in SAFe D samples (Xue et al., 2012; Conway et al., 2013). Additionally, external accuracy in seawater was demonstrated by strong agreement between our method and other labs for seawater dissolved δ^{114}Cd/$\varepsilon^{114/110}$Cd measurements across the full range of dissolved Cd concentrations encountered in the western North Atlantic (1–315 pmol kg^{-1}) on the GEOTRACES IC1 cruise (Boyle et al., 2012; Conway et al., 2013).

2.2.2. Particulate Cd, Ba and PO_4^{3-}

Particulate Cd, Ba and P concentrations were determined following a leaching procedure originally developed for determination of ligand-leachable (labile) δ^{56}Fe as described by Revels (2013). Briefly, 1/32nd portions of the originally 142 mm diameter polyethersulfone filters were cut using a ceramic blade and then leached with an oxalate-EDTA leach comprising of 0.1 mol L^{-1} oxalic acid and 0.05 mol L^{-1} EDTA in ultrapure water adjusted to pH 8 with reagent grade sodium hydroxide. Samples were leached in a polyethylene vial at 90 °C in an oven for 2 h and then filtered via a Norm-Ject polyethylene/polypropylene syringe and an uncleaned Whatman 0.45 μm PTFE Teflon filter membrane cartridge. Filtered leachate samples were diluted to 5% with 0.1 mol L^{-1} HNO_3 before analysis of Ba, Cd and P concentration by reference to standards in an identical matrix, using a Thermo Element II sector field ICPMS with a cyclonic spray chamber without desolvation, a ~150 μL min^{-1} PFA Teflon nebulizer and Ni sampler and Ni 'H' skimmer cones. Elemental concentrations were then converted to nmol L^{-1} by reference to the pumped volume for each filter divided by 32, assuming homogenous distribution of particulate matter. Uncertainty for particle concentrations was estimated as the sum of errors for 10% uncertainty due to variability in filter subsampling and a blank-correction uncertainty of 0.014, 0.00004 and 0.11 nmol L^{-1} for Ba, Cd and P, respectively.

Our measurements of particulate Ba, Cd and P concentration are in strong agreement with those made by Ohnemus and Lam (2014) on total HF digestions of subsamples of the same filters, suggesting that our leaching technique provides near-quantitative if not quantitative determination of these three elements. We are therefore confident that our particulate P, Cd and δ^{114}Cd are representative of the bulk suspended particles, and are not biased by selective leaching of different particulate phases.

2.3. Dissolved and particulate Cd*

Cd* is a parameter which highlights deviations in the relationship between Cd and PO_4^{3-} within the water column, as a result of preferential removal of either Cd or PO_4^{3-} relative to the other (e.g., Baars et al., 2014; Janssen et al., 2014); in this study we calculated both dissolved and particulate Cd* following Janssen et al. (2014) as:

$$\mathrm{Cd}^* = \mathrm{Cd}_{\mathrm{measured}} - \left(\mathrm{Cd}/\mathrm{P}_{\mathrm{deep}} \times \mathrm{P}_{\mathrm{measured}}\right)$$

where Cd is expressed in nmol kg^{-1} or L^{-1}, P in μmol kg^{-1} or L^{-1} and $\mathrm{Cd}/\mathrm{P}_{\mathrm{deep}}$ is set at 0.25 for the North Atlantic. We chose this North Atlantic value to make our figures and discussion comparable to Janssen et al. (2014). Particulate Cd* values are much smaller in magnitude than dissolved Cd* values, and are therefore expressed as $\times 10^{-3}$ for clarity.

2.4. Data processing

Data for figures was processed using an in-house interpolation scheme implemented in Matlab. First, values for all depths at each station were determined by 1-dimensional vertical linear interpolation, and then the vertically interpolated profiles were horizontally interpolated to provide a 2 dimensional ocean section. Replicate analyses at the same depth were averaged. Filtered seawater samples from within a hydrothermal plume which was sampled at USGT11-16 (the TAG hydrothermal field) are regarded as plume waters which are unlikely to mix laterally with adjacent stations due to the bathymetry of the ridge valley, and so are not included in sections for dissolved parameters, with the depth of exclusion (>2400 m) based on temperature and salinity anomalies. However, plume particulate samples are included within particulate section scatter plots.

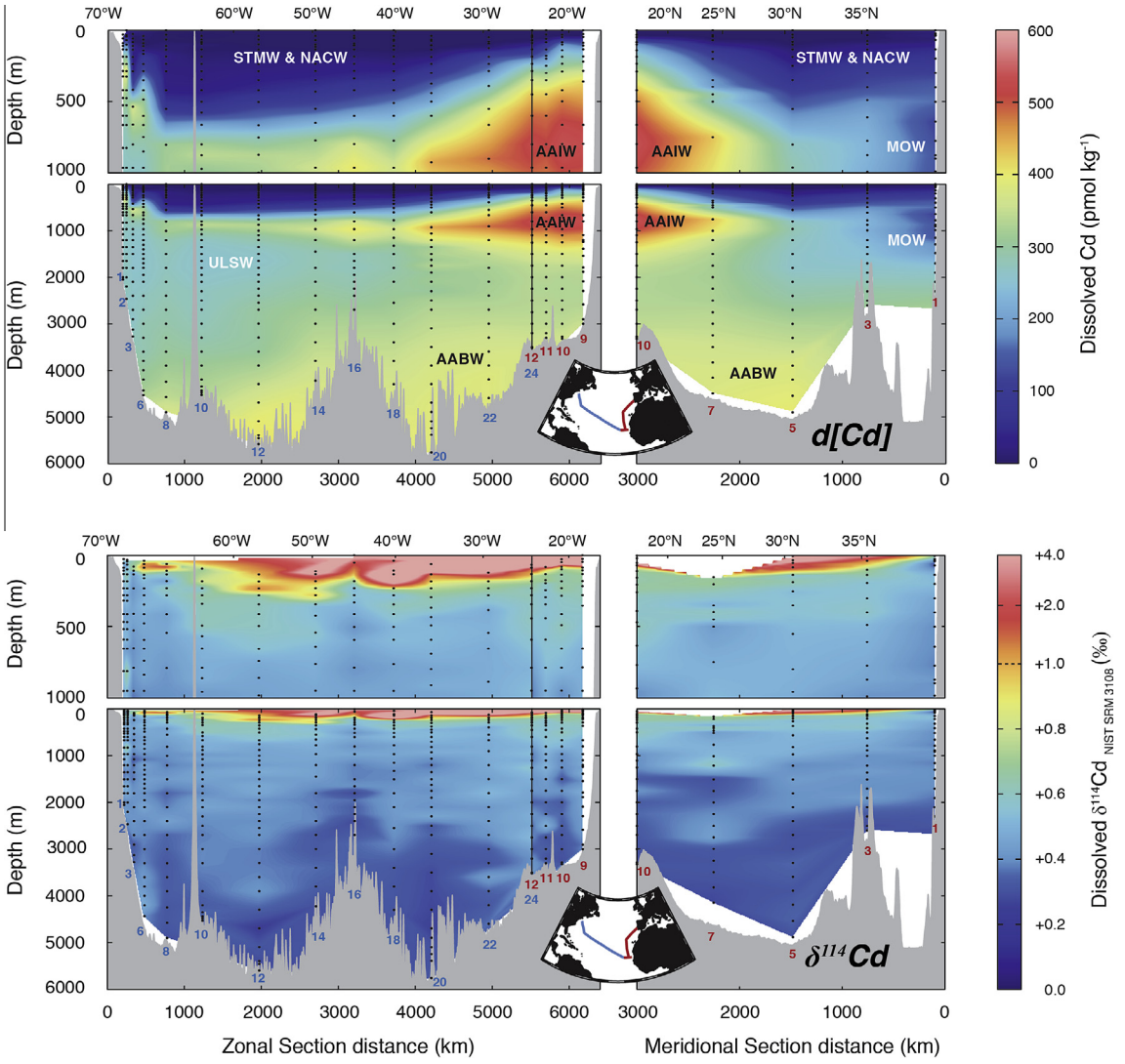

Fig. 2. Dissolved cadmium concentration (d[Cd]) and dissolved δ^{114}Cd along the GA03 North Atlantic section. The influence of major water-masses on dissolved Cd are shown as labels, with Antarctic-sourced water masses in black and North Atlantic water masses in white; Antarctic Intermediate Water (AAIW), Antarctic Bottom Water (AABW), Upper Labrador Sea Water (ULSW), Mediterranean Outflow Water (MOW), Subtropical Mode Water and North Atlantic Central Water (STMW & NACW). Water mass descriptions and positions are based on Jenkins et al. (2014). The vertical black line denotes the crossover between cruises USGT10 and USGT11. Note the non-linear scale for δ^{114}Cd. (For interpretation of the references to color in this figure legend, the reader is referred to the web version of this article.)

3. RESULTS AND DISCUSSION

The distributions of dissolved Cd concentrations and δ^{114}Cd across the US GEOTRACES GA03 North Atlantic section are shown in Fig. 2. A subset of this data (5 stations, top 2000 m) was previously published by John and Conway (2014). We used Jenkins et al. (2014)'s Optimum Multiparameter Analysis (OMPA) for the GA03 section as the basis for our water-mass distributions, with the core signatures of AABW and AAIW defined based on the characteristics of these water masses close to the equator (4°S). As such, they represent dilutions from the preformed water masses formed in the Antarctic. At the broad scale, across the entire section, the distribution of dissolved Cd and δ^{114}Cd can be mostly described by the mixing between different water masses and the effects of biological uptake and regeneration in the upper ocean. However, there are also regions of the section where other processes affect dissolved Cd and δ^{114}Cd, including the processes of Cd sulfide precipitation in the low-oxygen waters of the Mauritanian Oxygen Minimum Zone (OMZ) close to North Africa and scavenging of Cd to hydrothermal particles near the Mid-Atlantic Ridge.

3.1. Oceanographic setting and distribution of dissolved Cd and δ^{114}Cd

3.1.1. Distribution of dissolved Cd along the GA03 section

Similar to the major nutrients phosphate and nitrate (Jenkins et al., 2014), the distribution of dissolved Cd concentrations (Fig. 2) in the North Atlantic is controlled by

both the spatial distribution of different Antarctic and North Atlantic water masses, with different end-member dissolved Cd concentrations, and the *in situ* biological cycling of Cd in the surface ocean. Biological uptake and regeneration of Cd are ultimately responsible for the different end-member dissolved Cd concentrations found in different water masses in the deep ocean, with biological uptake resulting in the depletion of Cd in the surface of the North Atlantic. The biological assimilation of Cd by phytoplankton at the surface, and subsequent regeneration of Cd from sinking organic material leads to a strong vertical gradient in dissolved Cd concentration through the surface ocean. Over time, regeneration of organic matter leads to the accumulation of Cd at depth and as water masses age. Accumulation of regenerated Cd, together with variable pre-formed Cd concentrations in different water masses leads to large differences in Cd concentrations between young North Atlantic and older Antarctic-sourced water masses. Accordingly, the highest concentrations of dissolved Cd throughout the GA03 section (Fig. 2) were observed in deep waters with a large contribution of Antarctic Bottom water (AABW; ~400 pmol kg^{-1}) and in eastern subsurface waters dominated by Antarctic Intermediate Water (AAIW; ~540 pmol kg^{-1}). Younger North Atlantic water masses such as Upper Labrador Seawater (ULSW; ~260 pmol kg^{-1}; representative of North Atlantic Deep Water) and Mediterranean Outflow (MOW; $\leqslant$200 pmol kg^{-1}) contain relatively lower dissolved Cd concentrations. The lower Cd concentrations in AABW, compared to preformed AABW in the Antarctic (400 vs. 800 pmol kg^{-1}; Abouchami et al., 2014; Baars et al., 2014) reflect dilution with NADW, with AABW only constituting ~20–50% of deep water below 3000 m (Jenkins et al., 2014). Close to the surface of the ocean, Cd becomes dramatically depleted (<10 pmol kg^{-1}), reaching values as low as 0.03 pmol kg^{-1} in the west of the basin. This depletion, which corresponds to dissolved Cd concentrations up to four orders of magnitude lower than deep waters, is due in part to *in situ* biological incorporation of Cd into phytoplankton within the euphotic zone, and partly due to the proliferation of nutrient-poor Subtropical Mode Waters (STMW; Palter et al., 2005). STMW spreads throughout the upper 500 m of the western basin, and has low nutrient concentrations due to nutrient removal in low-latitude STMW source regions (Palter et al., 2005; Jenkins et al., 2014).

3.1.2. Distribution of dissolved $\delta^{114}Cd$

In contrast to the clear differences in dissolved Cd concentration between of the different water masses distributed throughout the North Atlantic, the end-member dissolved $\delta^{114}Cd$ values of these water masses show much less variability, and consequently water masses are not as easily differentiated by dissolved $\delta^{114}Cd$. In deep waters >3000 m, $\delta^{114}Cd$ values of +0.2‰ to +0.3‰ (Fig. 2) are indistinguishable from our previous dissolved $\delta^{114}Cd$ measurements at the SAFe site in the North Pacific (+0.3‰, 1000 m depth; Conway et al., 2013). These $\delta^{114}Cd$ values are also consistent with deep water values of +0.2‰ to +0.3‰ described from the Pacific, North Atlantic and Antarctic Oceans, despite a range of 400–1000 pmol kg^{-1} dissolved Cd (Ripperger et al., 2007; Xue et al., 2012, 2013; Conway et al., 2013; Abouchami et al., 2014). The Atlantic deep $\delta^{114}Cd$ values reflect the penetration of AABW, carrying a global deep ocean $\delta^{114}Cd$ signature close to +0.25‰ northwards. In contrast to the Southern (>50°S) and Pacific Oceans, where the water column below <500 m is characterized by relatively homogenous $\delta^{114}Cd$ (Conway, unpublished data; Ripperger et al., 2007; Xue et al., 2013; Abouchami et al., 2014), dissolved $\delta^{114}Cd$ in the North Atlantic is instead characterized by an increase towards the surface, similar to the pattern observed in $\delta^{30}Si$ (de Souza et al., 2012). A vertical gradient in $\delta^{114}Cd$ values from a minimum of 0.24 ± 0.06‰ in deep waters >3000 m to ~+0.4‰ at 1000 m and up to +1‰ near the base of the mixed layer is present right across the GA03 section (Fig. 2). This is consistent with previous data from the North Atlantic (Boyle et al., 2012; Xue et al., 2012; Conway et al., 2013). A similar vertical gradient in $\delta^{114}Cd$ at ~48°S in the South Atlantic by (Abouchami et al., 2014) suggests that this pattern may be characteristic of both the North and South Atlantic, compared to the Pacific.

Even higher $\delta^{114}Cd$ values are observed within the surface mixed layer across the section, reaching a maximum of +5‰ (Fig. 2), when dissolved Cd concentrations decline to <10 pmol kg^{-1} (Fig. 2). The increase in dissolved $\delta^{114}Cd$ towards very heavy values in the euphotic zone is coincident with the strong vertical gradient in dissolved Cd concentrations, a result of near-quantitative uptake of Cd into phytoplankton cells, and consistent with a biological preference for assimilation of lighter cadmium isotopes, which has been observed both in culture (Lacan et al., 2006; Horner et al., 2013; John and Conway, 2014) and in oceanic $\delta^{114}Cd$ data (Ripperger et al., 2007; Ho et al., 2009; Abouchami et al., 2011, 2014; Gault-Ringold et al., 2012; Yang et al., 2012; Conway et al., 2013; Xue et al., 2013). While such Cd depleted samples are prone to larger errors and analytical concerns, values of +2‰ to +4‰ are consistent with data from other similarly Cd-depleted regions of the ocean (Ripperger et al., 2007; Boyle et al., 2012; Xue et al., 2012; Conway et al., 2013), including the North Atlantic, increasing our confidence in these analyses.

We regard biological uptake to be the primary control on the large-scale distribution of $\delta^{114}Cd$ throughout the section, either directly where Cd is biological acquired within the surface North Atlantic, or indirectly as water masses with different $\delta^{114}Cd$ signatures are brought to the North Atlantic by large-scale ocean circulation (Abouchami et al., 2014). The very depleted $\delta^{114}Cd$ signatures (>+0.7‰) of the mixed layer and STMW above 500 m are likely to be the result of biological incorporation of light Cd and incomplete regeneration, either happening *in situ* or in STMW source regions. Deeper in the water column, the vertical gradient in $\delta^{114}Cd$ likely reflects the mixing of AABW (+0.25‰, <3000 m), AAIW (+0.4‰ to +0.5‰ in this section, ~500–1500 m), and North Atlantic water masses, such as ULSW (NADW) and MOW. Both these North Atlantic water masses are characterized by dissolved $\delta^{114}Cd$ of +0.4‰ to +0.5‰. The heavier dissolved $\delta^{114}Cd$ signature in AAIW reflects the loss of isotopically light

Cd due to biological uptake and incomplete regeneration of Cd in Antarctic source regions where AAIW is characterized by +0.46‰ (Xue et al., 2013; Abouchami et al., 2014). Similarly, the depleted Cd signature of NADW likely reflects the more fractionated δ^{114}Cd of shallow North Atlantic source regions. In these regions, *in situ* biological fractionation and Cd supplied by water masses such as AAIW and STMW (with heavier δ^{114}Cd signatures) impart a heavy δ^{114}Cd signature to sinking NADW, analogous to that described for δ^{30}Si (de Souza et al., 2012).

3.1.3. Interaction of δ^{114}Cd and Zn

Abouchami et al. (2014) previously suggested an inverse relationship between δ^{114}Cd and dissolved Zn concentration in the surface Southern Ocean, with Cd being used in place of Zn within cells as Zn becomes depleted, leading to heavier δ^{114}Cd in surface waters. A similar relationship between δ^{114}Cd and Zn concentration is observed for our North Atlantic data (this study; John and Conway, 2014; Conway and John, 2014b), but here the relationship could simply be explained by coincident depletion of Cd and Zn concentrations towards the surface, with Zn and Cd up to four orders of magnitude lower in the euphotic zone compared to deeper waters in the North Atlantic (this study; Conway and John, 2014b).

3.1.4. Temporal variability in dissolved Cd and δ^{114}Cd

Three separate US GEOTRACES cruises in the North Atlantic during 2008–2011 have provided repeat occupation of two separate stations at different times, allowing us to assess the temporal variability in dissolved Cd and δ^{114}Cd. Fig. 3 shows a comparison of dissolved Cd concentrations and dissolved δ^{114}Cd at the crossover station in the Eastern Atlantic between USGT11 and USGT10 (USGT10-12, USGT11-24; 17.4°N, 24.5°W) and also at the Bermuda Atlantic Time Series station (31.8°N, 64.2°W) in the Western North Atlantic in the Western Atlantic which was sampled on both USGT11 and the GEOTRACES IC1 cruise in 2008, which was previously the subject of a trace-metal isotope intercomparison exercise (Boyle et al., 2012).

At the Bermuda Atlantic Time Series station, profiles from the IC1 (August 2008) and USGT11 (November 2011) are identical within 2σ error for dissolved δ^{114}Cd (Fig. 3), indicative of negligible temporal variability within the water column between the two cruises, suggesting the processes which control dissolved δ^{114}Cd in the Western North Atlantic are largely stable on this timescale. Dissolved Cd concentrations show similarly good agreement, except between 250 and 500 m, where differences may be due to seasonal differences in nutrient cycling, to a shallowing in the sub-surface Cd maximum associated with AAIW (Fig. 2) in 2008 compared to 2011 or to slight vertical error in sampling depth across an interval where dissolved Cd concentrations change dramatically. Salinity data from both cruises is supportive of a slight (~30 m) shallowing of the influence of AAIW in 2008 compared to 2011 (John and Adkins, 2012; Jenkins et al., 2014).

In the Eastern Atlantic, dissolved Cd concentrations are practically indistinguishable between 2010 and 2011, whilst dissolved δ^{114}Cd appears to show slight variability between the cruises, with similar shaped profiles but with USGT10-12 systematically offset by ~0.1‰ towards heavier δ^{114}Cd values between 250 and 3200 m depth. Whilst these differences are mostly within 2σ error, the systematic offset between years could point to real variability in the

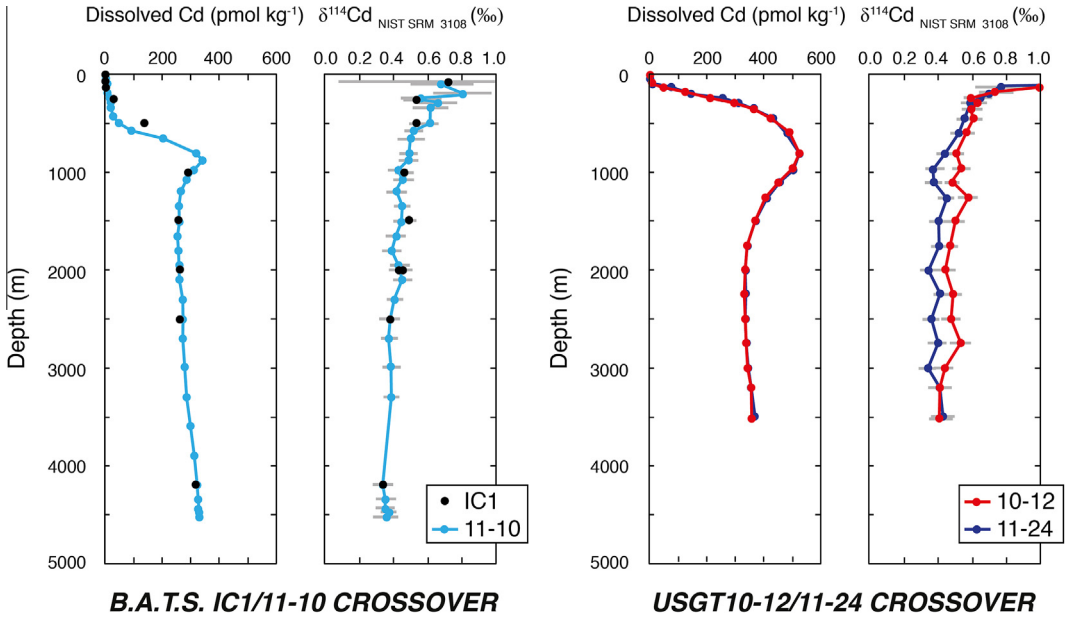

Fig. 3. Temporal variability of dissolved cadmium concentration and dissolved δ^{114}Cd in the North Atlantic. Data from the authors are shown both for the crossover station between USGT11-10 (October 2011; this study) and the GEOTRACES IC1 cruise (August 2008; Conway et al., 2013) at the Bermuda Atlantic Time Series station (BATS; 31.8°N, 64.2°W), and for the crossover station on the GA03 section (USGT10-12, USGT11-24; 17.4°N, 24.5°W). (For interpretation of the references to color in this figure legend, the reader is referred to the web version of this article.)

processes controlling dissolved δ^{114}Cd in this region of the North Atlantic. Variability on this time scale is also evident for both Fe and Zn, with variability of up to 20% in dissolved Fe concentration and up to 0.2‰ in δ^{56}Fe between the two cruises (Conway and John, 2014a; Conway and John, 2014b). There are more pronounced horizontal gradients in dissolved δ^{114}Cd within the eastern basin (Fig. 2), meaning that δ^{114}Cd in the east of the North Atlantic may be far more sensitive than δ^{114}Cd in the western basin to either the varying importance of AAIW supplying Cd at +0.4‰ to 0.5‰ (this study; Abouchami et al., 2014), or to a change in the influence of the Cd sulfide precipitation within low-oxygen waters of the Mauritanian OMZ (Section 3.2).

3.2. Cd sulfide precipitation in low oxygen waters

Recently, using Cd data from just two of the stations presented here (USGT10-9 and USGT11-14), we hypothesized that Cd sulfides are precipitated in micro-environments around sinking biogenic particles. Notably, it was suggested that this takes place within the water column in regions where dissolved oxygen concentrations are low (<75 μmol kg^{-1}), but not anoxic or sulfidic (Janssen et al., 2014). Evidence for Cd sulfide precipitation in the low-oxygen waters of the Mauritanian OMZ (~45 μmol kg^{-1}) in the eastern part of the North Atlantic section included: (1) an observed deficit in dissolved Cd relative to dissolved PO_4^{3-} (negative dissolved Cd*), (2) high particulate Cd concentrations not associated with high concentrations of particulate biological PO_4^{3-} (high particulate Cd*), and (3) particulate δ^{114}Cd as light as −0.01‰ when biogenic particulate Cd would be expected to reflect the dissolved δ^{114}Cd of the mixed layer (+0.8‰). The supporting data for Cd sulfide precipitation from Janssen et al. (2014) are collated in Fig. 4. In this present manuscript, we expand upon Janssen et al.'s earlier discussion of those lines of evidence with new data from the rest of the GA03 section. We also present new lines of evidence, including the distribution of particulate Ba and particulate Cd*. The effects of Cd sulfide precipitation on the distribution of Cd and δ^{114}Cd along the GA03 section are subtle, and have a much less noticeable impact than water mass mixing and biological cycling (Section 3.1). However, a Cd sulfide removal process is important to consider because of the role it could play as an important sink for Cd on timescales longer than the residence time of Cd in the ocean (thousands of years), and thus it may influence both δ^{114}Cd and the relationship between marine dissolved Cd and PO_4^{3-} on geological timescales.

3.2.1. Dissolved δ^{114}Cd and oxygen concentrations in the Mauritanian OMZ

Janssen et al. (2014) inferred that Cd sulfide precipitation represented a sink of isotopically light Cd from the oceans, based in part on the light δ^{114}Cd signature of particles formed within the Mauritanian OMZ at USGT10-9 (Fig. 4). Here, we present the first direct evidence that dissolved Cd in low-oxygen waters of the North Atlantic is left isotopically heavier as a result of Cd sulfide precipitation within the water column. As described earlier, most of the variability in dissolved Cd concentration and δ^{114}Cd observed throughout the GA03 section can be ascribed to water-mass mixing, fractionation during biological uptake and regeneration of Cd (Sections 3.1.1 and 3.1.2). However, a closer examination of the relationship between dissolved Cd concentration and δ^{114}Cd reveals that for similar Cd concentrations, δ^{114}Cd are consistently heavier in low-oxygen waters than in high-oxygen waters (Fig. 5). In fact, there appears to be a fairly consistent trend between dissolved oxygen concentration and dissolved δ^{114}Cd. Among all of the samples with high dissolved Cd concentrations (>200 pmol kg^{-1}), the lightest dissolved δ^{114}Cd values are observed for samples with the highest dissolved oxygen concentration (>150 μmol kg^{-1}). Equally, the heaviest dissolved δ^{114}Cd values are observed at the lowest dissolved oxygen concentrations (<100 μmol kg^{-1}).

The observed pattern (Fig. 5) is not consistent with either a water mass or biological signal. Dissolved δ^{114}Cd values in the low-oxygen region are heavier than would be expected from either AAIW or AABW end-members, which are the main sources of Cd to the region (Fig. 5). Biological uptake of Cd in the surface ocean in this region of the ocean is nearly quantitative, so biological uptake and regeneration should not have any net impact on dissolved δ^{114}Cd at depth. Because of the depth gradient in δ^{114}Cd in the upper ocean, it is probable that biogenic material regenerating deep in the thermocline has a higher δ^{114}Cd than ambient dissolved δ^{114}Cd, and thus regeneration could lead to an increase in δ^{114}Cd. However, this process cannot explain why δ^{114}Cd is so high just below the mixed layer, and in deeper waters it should lead to a concomitant increase in Cd concentration, which is at odds with negative Cd* data.

3.2.2. Dissolved δ^{114}Cd and Cd* in low-oxygen waters

Cd*, as used by several authors (e.g., Baars et al., 2014; Janssen et al., 2014) is a parameter that highlights how dissolved Cd may be enriched or depleted relative to PO_4^{3-}. For the GA03 section, we calculated Cd* for both dissolved and particulate Cd following Janssen et al. (2014), setting the deep Atlantic to Cd:PO_4^{3-} to 0.25 nmol μmol^{-1} (Section 2.3; Figs. 4–6). Dissolved Cd* values are close to 0 across the section, with most between −0.05 to +0.05, reflecting the variable influence of different water masses. For example, dissolved Cd* in waters influenced by AABW is noticeably higher (+0.02) than for regions influenced by AAIW (−0.02 to −0.04) and northern water masses such as ULSW and NADW (−0.04). Differences in Cd* between AAIW and AABW in the Antarctic have previously been attributed to the preferential biological uptake of Cd over PO_4^{3-} in the surface Southern Ocean (Baars et al., 2014). In the North Atlantic, a combination of advected Antarctic Cd* signals, regeneration associated with the eastern OMZ and mixing of different water masses are likely to influence the Cd* signatures of AABW and AAIW.

In the east of the GA03 section, just below the surface mixed layer (<50 m) and at the top of the Mauritanian OMZ, we observe a dramatic negative excursion in dissolved Cd* associated with low dissolved oxygen

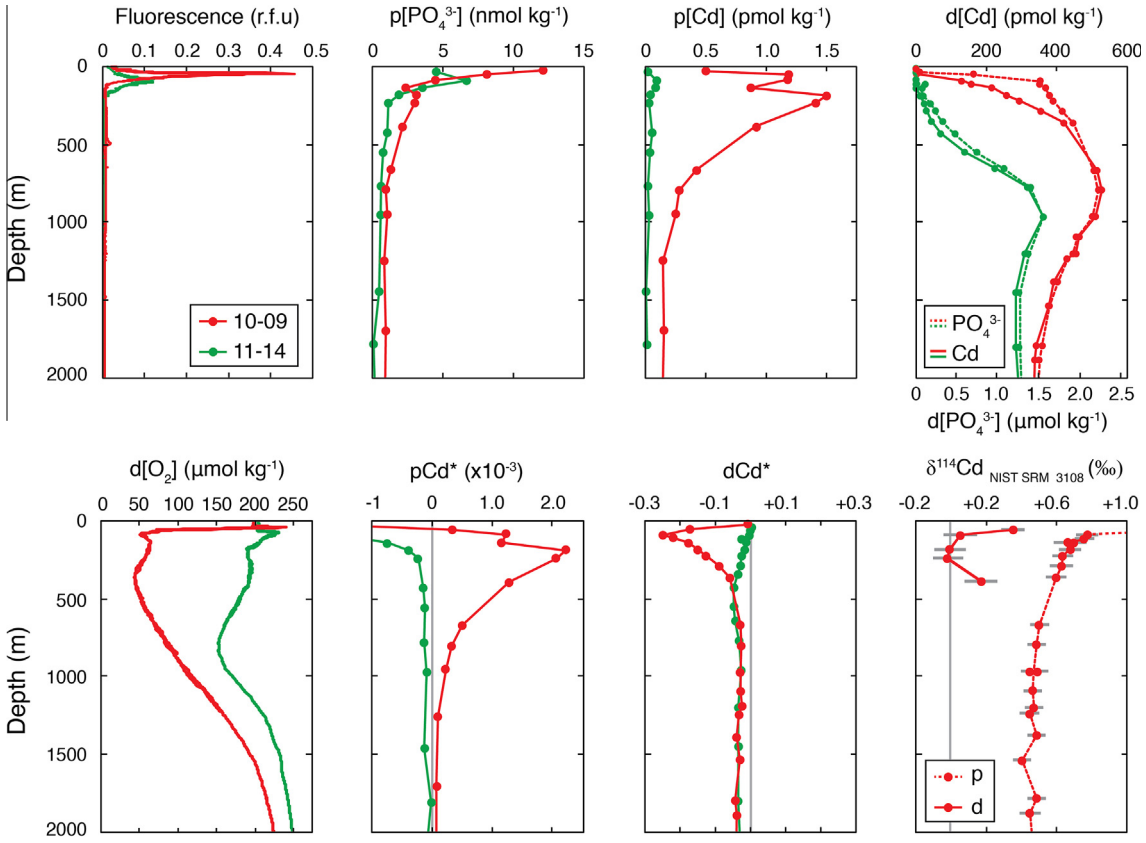

Fig. 4. Previously published dissolved and particulate evidence for cadmium sulfide precipitation within the Mauritanian oxygen minimum zone in the North Atlantic (Janssen et al., 2014). Dissolved oxygen (d[O_2]), dissolved and particulate Cd concentration (d[Cd], p[Cd]); dissolved Cd^* (dCd^*), dissolved and particulate phosphate (d[PO_4^{38}]), p[PO_4^{3-}]), and dissolved (d) and particulate (p) $\delta^{114}Cd$ are shown based on Figs. 2 and 3 of Janssen et al., 2014. Data are from stations USGT10-9 (17.4°N 18.25°W; red) and USGT11-14 (27.6°N 49.6°W; green) are shown. Particulate Cd^* (pCd^*) and dissolved $\delta^{114}Cd$ (1500–2000 m) are also shown from this study. Fluorescence is shown in relative fluorescence units (r.f.u). (For interpretation of the references to color in this figure legend, the reader is referred to the web version of this article.)

concentrations (Figs. 4 and 6). This region of extremely low dissolved Cd^* values (<−0.1) extends from West Africa as far west as ~35°W and as far north as ~30°N, with values reaching a minimum of −0.24 at USGT10-10 (85 m) and −0.25 at USGT10-9 (89 m), where oxygen is <60 µmol kg^{-1}. These negative dissolved Cd^* values represent a significant deficit of dissolved Cd relative to dissolved PO_4^{3-}. In fact, 20–60% of the expected dissolved Cd is 'missing' within the top 80–300 m at USGT10-9 and USGT10-10 and as much as 80% is missing between 80 and 250 m at USGT10-11 and USGT11-12, assuming background dissolved Cd^* being 0 to −0.03 in this region. A subtle minimum in dissolved Cd^* (−0.05 to −0.15) can be observed right across the entire GA03 section, tracking the subsurface low-oxygen minimum, including the shallower region of lower oxygen close to North America (Fig. 6).

Instead of Cd sulfide precipitation, an alternative explanation for the negative dissolved Cd^* observed in the east of the section could be that the dissolved Cd^* signal originates in the Southern Ocean and results from the preferential uptake of Cd compared to PO_4^{3-} in surface Antarctic waters forming AAIW (Baars et al., 2014). However, several lines of evidence show that AAIW is not responsible for the observed negative dissolved Cd^* values. Firstly, the core of AAIW is present at around 600–2000 m depth close to the African margin, where dissolved Cd^* is −0.02 to −0.04, whilst the much more negative dissolved Cd^* values are at depths of 80–300 m. Secondly, the difference in Cd/PO_4^{3-} described for the AAIW end member in the Antarctic is ~0.05 nmol µmol^{-1} (AABW–AAIW; Baars et al., 2014), which is not large enough to explain the North Atlantic data, which instead correspond to a Cd/PO_4^{3-} deficit of up to ~0.2 nmol µmol^{-1}. In fact, the preformed AAIW end member in the Antarctic, with a Cd/PO_4^{3-} of 0.32 nmol µmol^{-1} (Baars et al., 2014) would have a positive Cd^* using our equation. Thirdly, the Cd/P of the 'AAIW' water mass present in the section is likely to have been modified by both dilution with other water masses and the influence of regeneration within the OMZ, and does not correspond to pure AAIW.

The possibility of negative dissolved Cd^* resulting from the addition of PO_4^{3-} from shelf sediments, or loss of Cd to shelf sediments, was considered and discounted by Janssen et al. (2014), based on both the spatial location of the dissolved Cd^* signal, which is high within the water-column, not close to margin sediments, and also by reference to

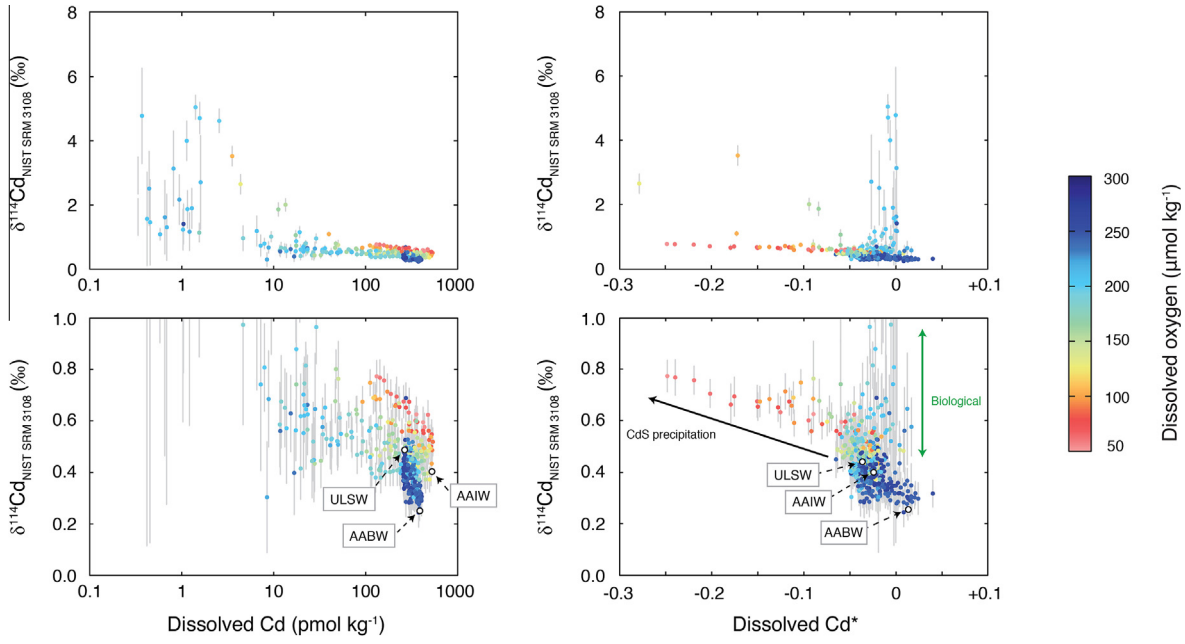

Fig. 5. The influence of biological uptake and cadmium sulfide precipitation on dissolved $\delta^{114}Cd$ in the North Atlantic. Dissolved $\delta^{114}Cd$ are shown plotted against either dissolved cadmium concentration or dissolved Cd^*, with the color of points indicating dissolved oxygen concentration (μmol kg^{-1}) and gray bars indicating 2σ error. Dissolved Cd^* is as calculated in the text. At the broad scale, we regard most dissolved Cd concentrations and $\delta^{114}Cd$ as being a result of mixing of Antarctic Bottom Water (AABW) or Antarctic Intermediate Water (AAIW), and Northern Atlantic water masses (represented by Upper Labrador Seawater, ULSW), or biological fractionation in the surface ocean. Representative water mass compositions are shown for AAIW (540 pmol kg^{-1} Cd, $\delta^{114}Cd$ of +0.4‰, Cd^* of −0.02), AABW (400 pmol kg^{-1} Cd, $\delta^{114}Cd$ of +0.25‰, Cd^* of +0.02) and ULSW (260 pmol kg^{-1}, $\delta^{114}Cd$ of 0.45‰, Cd^* of −0.04). These representative end-members are based on measured values in the GA03 section rather than preformed Antarctic signatures. Thus, the water mass labeled AABW here reflects a ~1:1 dilution with North Atlantic water masses (Jenkins et al., 2014). Arrows indicate approximate fractionation of $\delta^{114}Cd$ and change in Cd^* due either to Cd sulfide precipitation or biological uptake, with near-quantitative biological incorporation of Cd and phosphate into phytoplankton in surface waters with a near-oceanographic Cd/phosphate ratio inducing no change in Cd^*. (For interpretation of the references to colour in this figure legend, the reader is referred to the web version of this article.)

$\delta^{56}Fe$ measurements which trace reduced pore-water inputs to the water column and show them to be strongest at the base of the water column, not in the region where the negative dissolved Cd^* is observed (Conway and John, 2014a). Additionally, the new data presented here clearly show the dissolved Cd^* signal extending far from the margin, right across the basin, corresponding most clearly to oxygen deficient waters and not a direct sedimentary influence.

Similar to the observation that dissolved $\delta^{114}Cd$ is elevated within low-oxygen waters within the Mauritanian OMZ (Section 3.2.1), dissolved $\delta^{114}Cd$ is also elevated in regions of negative dissolved Cd^*. This can be best observed by comparing dissolved Cd^* with dissolved $\delta^{114}Cd$ (Fig. 5). Whilst biological processes can have a large impact on dissolved $\delta^{114}Cd$, they leave dissolved Cd^* relatively unchanged because both Cd and PO_4^{3-} are nearly quantitatively depleted by biological uptake in the mixed layer, as demonstrated by dissolved Cd^* values of ~0 at the surface across the GA03 section. Thus, on a dissolved Cd^*/dissolved $\delta^{114}Cd$ plot, biological fractionation in the surface ocean leads to data characterized by an approximately vertical line. As expected, we see that variability in the relationship between Cd^* and $\delta^{114}Cd$ occurs primarily in the vertical direction for high-oxygen waters. There is also slight horizontal variability in Cd^* from water mass mixing between marked water mass end members with slightly different preformed Cd^* (Fig. 5). In low oxygen waters, however, there is a much larger decrease in dissolved Cd^*, which is associated with a trend towards higher dissolved $\delta^{114}Cd$ (Fig. 5). The vector is consistent with the precipitation of Cd sulfides that are isotopically lighter than the surrounding waters.

3.2.3. Particulate Cd^* and Ba in low-oxygen waters

A final line of evidence supporting the precipitation of Cd sulfide within the water column in low-oxygen waters of the Mauritanian OMZ is new data on particulate Cd^* and particulate Ba concentration. As with dissolved Cd^*, particulate Cd^* is not expected to change based on biological uptake and regeneration because phytoplankton incorporate both Cd and PO_4^{3-} with a ratio close to deep ocean Cd/PO_4^{3-}. Indeed, we observe that particulate Cd^* is less than $+0.05 \times 10^{-3}$ throughout most of the GA03 section (Fig. 6). Within the low-oxygen waters of the Mauritanian OMZ, however, particulate Cd^* reach values as high as $+2.2 \times 10^{-3}$ (Figs. 4 and 6). The highest particulate Cd^* values are observed at depths of 80–600 m in the four stations closest to the African Margin, within the OMZ. These values are at, or just below, the depths within the OMZ where the most negative dissolved Cd^* values along the

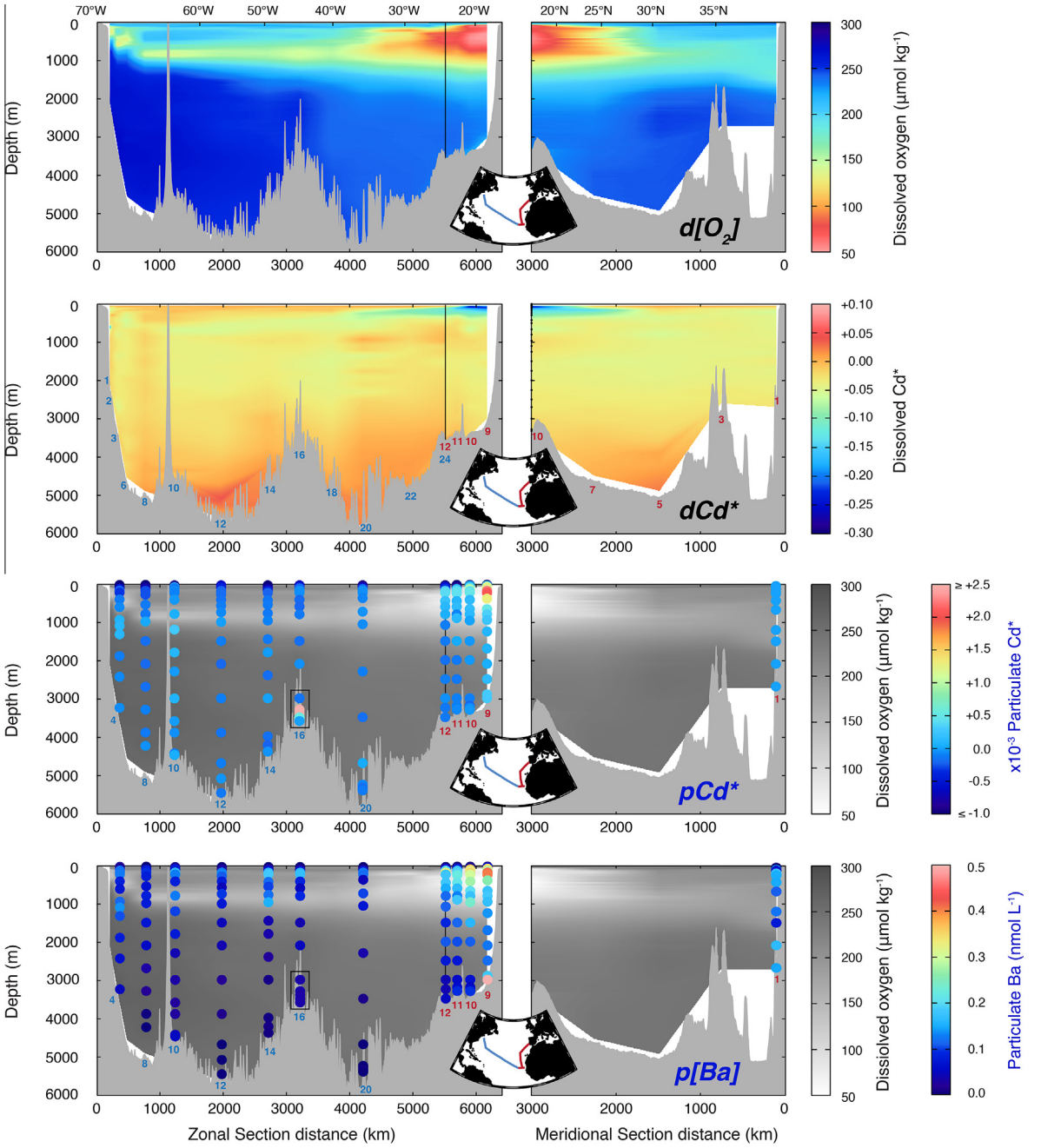

Fig. 6. The influence of low-oxygen waters on the marine cadmium cycle along the GA03 North Atlantic Section. Dissolved oxygen (d[O_2]; µmol kg^{-1}), dissolved and particulate Cd^* (see text for details) and particulate barium (p[Ba]; nmol L^{-1}) are shown, illustrating the minimum in dissolved Cd^* coincident with the oxygen minimum region and maxima in particulate Cd^* and particulate barium. The vertical black line denotes the crossover between cruises USGT10 and USGT11. The black boxes denote samples from within a hydrothermal plume at the TAG hydrothermal site (USGT11-16); see Fig. 7. Both dissolved and particulate Cd^* are as calculated in the text. (For interpretation of the references to color in this figure legend, the reader is referred to the web version of this article.)

GA03 section are observed (~80–300 m; Figs. 4 and 6). The pairing of these datasets is clearly suggestive of a transfer of Cd from the dissolved to the particulate phase as dissolved oxygen concentrations decline into the top of the OMZ. We note that the supply of both Cd and PO_4^{3-} from aerosol dust would be expected to drive particulate Cd^* to negative values, due to the much smaller Cd/PO_4^{3-} ratio of lithogenic particles (Taylor, 1964; Ho et al., 2009), and therefore could not be responsible for the maximum in particulate Cd^* observed here. Indeed, dust may be responsible for the more negative particulate Cd^* seen in the very surface waters across the section (Fig. 6).

Particulate data also provides more insight into the mechanism by which Cd may be transferred to the particulate phase. Janssen et al. (2014) proposed that Cd was precipitated with sulfides in anoxic microenvironments

surrounding biogenic particles. These environments are analogous to the isolated microenvironments associated with sinking organic matter where marine barites are thought to form (Bishop, 1988; Wright et al., 2012). Here we show that particulate Ba concentrations also have a similar distribution to particulate Cd^*, with high particulate Ba concentrations observed in samples with high particulate Cd^* (Fig. 6), strongly supporting the hypothesis that both particulate Ba and Cd sulfides are formed in isolated microenvironments around biogenic particles. Across the North Atlantic section, evidence for Cd sulfide and Ba precipitation (high particulate Cd^* and Ba) is observed most strongly at the top of the Mauritanian OMZ, instead of throughout the full depths of the OMZ (where oxygen is $<100\ \mu mol\ kg^{-1}$). We attribute this pattern to the rapid regeneration of biogenic particles as they sink through the water column, with particulate PO_4^{3-} concentrations decreasing by nearly an order of magnitude in the upper ~500 m of the North Atlantic (Janssen et al., 2014; Ohnemus and Lam, 2014). If both Cd sulfide and Ba are precipitated in low-oxygen microenvironments associated with biogenic particles, then the highest rates of precipitation will be observed where there is a combination of low water column dissolved oxygen concentrations, and a high concentration of biogenic particulate material, as is observed in our data.

Data from the North Atlantic GA03 section provides some insight into whether Cd sulfide formed within low-oxygen waters of the Mauritanian OMZ is exported to and buried in deep sediments, where it could be an important sink of Cd from the oceans. While the data presented here are for the suspended phase (0.8–51 μm), suspended phase particles are generally thought to be in equilibrium with larger particles through adsorption, providing a mechanism by which suspended CdS could be transported to sediments (Bacon and Anderson, 1982). Elevated particulate Cd^* and Ba throughout the water column at USGT10-9 and as deep as ~1500 m at USGT10-10 suggest that particulate Cd sulfides persist in sinking particles even outside low-oxygen waters, and are therefore likely to reach ocean floor sediments.

3.3. The influence of Mid-Atlantic Ridge Vents on dissolved cadmium

Above the TAG black-smoker site on the Mid-Atlantic Ridge (26.1°N, 44.8°W), a hydrothermal plume was directly sampled as part of USGT11-16 (Fig. 7). Whilst Atlantic black smoker hydrothermal vents are sources of metals such as Fe and Zn to the ocean (e.g. Saito et al., 2013; Conway and John, 2014a; Conway and John, 2014b), dissolved Cd within the TAG plume is noticeably depleted relative to the non-hydrothermally influenced background at flanking stations USGT11-14 and USGT11-18 (Fig. 7). The homogeneity of the deep Atlantic Ocean for dissolved Cd concentration across these stations allows us to calculate a Cd loss for the depths within the hydrothermal plume at USGT11-16 of between 3% and 23% or 11–77 $pmol\ kg^{-1}$, against a background of 320–340 $pmol\ kg^{-1}$. Dissolved $\delta^{114}Cd$ is fractionated compared to the deep-ocean background dissolved $\delta^{114}Cd$ at these depths (+0.36‰ to +0.37‰), with $\delta^{114}Cd$ values within the hydrothermal plume waters as heavy as $+0.55 \pm 0.07$‰. The data is most simply explained by scavenging of isotopically light Cd scavenging onto plume particles (Fig. 7). Particles are likely to be largely comprised of precipitated Fe oxyhydroxides which have been previously shown to readily scavenge Cd even at high ambient dissolved oxygen concentrations (German et al., 1991), and scavenged Cd may be in the form of Cd sulfides, as has been previously observed for other metals (Klevenz et al., 2011). Measurements of $\delta^{114}Cd$ in sulfides from black smoker chimneys in the Pacific are all close to +0.05‰ (Schmitt et al., 2009, converted in Rehkämper et al., 2012), consistent with both a MORB ocean crust $\delta^{114}Cd$ signature of 0.00 ± 0.03‰ and precipitation/scavenging of Cd to particles with a lighter-than-seawater $\delta^{114}Cd$ signature. For this reason, we do not think that the changes in dissolved $\delta^{114}Cd$ within the hydrothermal plume represent an input of isotopically heavy Cd from hydrothermal fluids. Instead, hydrothermal systems in the North Atlantic are likely to constitute a removal process for isotopically light Cd from the dissolved phase, thus constituting a global sink for Cd from the oceans. However, given that the observed dissolved Cd anomalies are restricted to samples collected from within the hydrothermal plume, and are not apparent at nearby stations, it seems unlikely that this process has a significant effect on the overall dissolved ocean Cd reservoir.

4. IMPLICATIONS FOR THE GLOBAL MARINE CD CYCLE AND CONCLUSIONS

Understanding the role that Cd occupies in modern biogeochemical cycles, especially the marine carbon cycle, relies on a firm understanding of the processes which influence both the size and isotopic signature of the dissolved Cd reservoir in the oceans. Accurate constraints on the oceanic sinks and sources of Cd are key to assessments of the marine Cd cycle, as well as being vital to the use of either Cd/Ca or $\delta^{114}Cd$ as tracers of past ocean processes. Factors such as continental configuration, ocean circulation and global climate are likely to influence the global distribution of low-oxygen waters on geological timescales, and thus affect the amount of Cd which is removed from the oceans by sulfide precipitation. A global Cd sulfide sink that is isotopically lighter than riverine inputs to the ocean may also explain why the $\delta^{114}Cd$ signature of the global oceanic dissolved Cd reservoir is isotopically heavier than riverine Cd inputs by ~0.2‰. Relative changes in the balance of riverine inputs and various Cd sinks may therefore influence global ocean $\delta^{114}Cd$. For example, changes in the size of an oceanic Cd sulfide sink could lead to variability in both the global dissolved Cd/PO_4^{3-} relationship and the $\delta^{114}Cd$ of the deep ocean dissolved Cd reservoir on long timescales. Most studies of the processes that affect dissolved Cd/PO_4^{3-} have focused on biological Cd uptake in the high-latitude surface oceans. At high latitudes, differential partitioning of Cd and PO_4^{3-} between dissolved and particulate

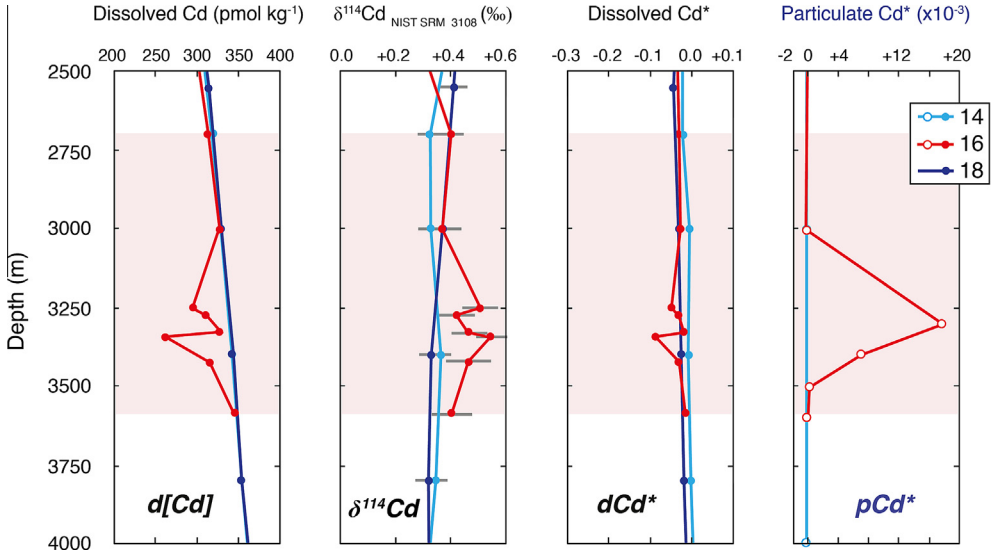

Fig. 7. The influence of the Mid-Atlantic Ridge on dissolved cadmium. Data are shown for samples collected within a hydrothermal plume at station USGT11-16 at the TAG site on the Mid-Atlantic Ridge (26.1°N, 44.8°W), as well as nearby flanking stations USGT11-14 (27.6° 49.6°) and USGT11-18 and (24.14° 40.2°). The shaded red bar indicates the depth interval which is influenced by the hydrothermal plume at USGT11-16, based on temperature and salinity anomalies. Error bars are 2σ as calculated in the text. (For interpretation of the references to colour in this figure legend, the reader is referred to the web version of this article.)

reservoirs may lead to different preformed Cd/ PO_4^{3-} ratios in different water masses (e.g., Elderfield and Rickaby, 2000; Baars et al., 2014). However, processes such as Cd sulfide formation, which occur at low-latitudes may also be influential in determining the global Cd/PO_4^{3-} relationship.

Here, we have presented a high-resolution paired ocean section of dissolved Cd and δ^{114}Cd from the US GEOTRACES GA03 section through the North Atlantic Ocean. Using this dataset we have shown that whilst biological cycling and large-scale mixing of different water masses and are the dominant processes that influence the distribution of Cd and δ^{114}Cd in the North Atlantic, both dissolved and particulate data are consistent with the precipitation of Cd sulfides within low oxygen waters of the North Atlantic. We anticipate that assessing the magnitude of a marine Cd sulfide sink and its affects on both global dissolved δ^{114}Cd and Cd/PO_4^{3-} will be the focus of future studies that will make use of 3-dimensional modeling. Further oceanic Cd and δ^{114}Cd datasets will help to constrain estimates of Cd sulfide fluxes to sediments and to determine how large regions of low-oxygen found in both Pacific and Indian oceans affect global δ^{114}Cd and Cd*. Such studies are likely to be essential to use of Cd/Ca as a nutrient proxy in the past, as well as the development of δ^{114}Cd and other redox-sensitive metals such as δ^{66}Zn as proxies for past oceanic processes.

ACKNOWLEDGMENTS

We thank the Captain, crew and GEOTRACES water sampling and pumping teams on board the R/V Knorr on both USGT10 and USGT11 cruises, and Phoebe Lam and Daniel Ohnemus for providing particulate samples. We also thank Brandi Revels, Florence Hartman, Angela Rosenberg and Beth Bair for technical assistance at USC, Ken Bruland, Rob Middag and Jingfeng Wu for supplying concentration data that informed double-spike calculations. The Ocean Data Facility supplied macronutrients and oceanographic parameters from the cruises, and we thank Bill Jenkins and coauthors for water mass analysis (OMPA). We thank Associate Editor Claudine Stirling, Gregory de Souza and two anonymous reviewers for their insightful comments that allowed us to improve this manuscript. This study was funded by the University of South Carolina and National Science Foundation Grant OCE-1131387.

APPENDIX A. SUPPLEMENTARY DATA

Supplementary data associated with this article can be found, in the online version, at http://dx.doi.org/10.1016/j.gca.2014.09.032.

REFERENCES

Abouchami W., Galer S. J. G., De Baar H. J. W., Alderkamp A. C., Middag R., Laan P., Feldmann H. and Andreae M. O. (2011) Modulation of the Southern Ocean cadmium isotope signature by ocean circulation and primary productivity. *Earth Planet. Sci. Lett.* **305**(1–2), 83–91. http://dx.doi.org/10.1016/j.epsl.2011.02.044.

Abouchami W., Galer S. J. G., Horner T. J., Rehkämper M., Wombacher F., Xue Z., Lambelet M., Gault-Ringold M., Stirling C. H., Schönbächler, Shiel A. E., Weis D. and Holdship P. F. (2013) A common reference material for cadmium isotope studies – NIST SRM 3108. *Geostand. Geoanal. Res.* **37**(1), 5–17. http://dx.doi.org/10.1111/j.1751-908X.2012.00175.x.

Abouchami W., Galer S. J. G., De Baar H. J. W., Middag R., Vance D., Zhao Y., Klunder M., Mezger K., Fedlmann H. and Andreae M. O. (2014) Biogeochemical cycling of cadmium isotopes in the Southern Ocean along the Zero Meridian. *Geochim. Cosmochim. Acta* **127**, 348–367. http://dx.doi.org/10.1016/j.gca.2013.10.022.

Baars O., Abouchami W., Galer S. J. G., Boye M. and Croot P. L. (2014) Dissolved cadmium in the Southern Ocean: distribution, speciation, and relation to phosphate. *Limnol. Oceanogr.* **59**(2), 385–399. http://dx.doi.org/10.4319/lo.2014.59.2.0385.

Bacon M. P. and Anderson R. F. (1982) Distribution of thorium isotopes between dissolved and particulate forms in the deep sea. *J. Geophys. Res.: Oceans* **87**(C3), 2045–2056. http://dx.doi.org/10.1029/JC087iC03p02045.

Biller D. V. and Bruland K. W. (2012) Analysis of Mn, Fe Co, Ni, Cu, Zn, Cd, and Pb in seawater using the Nobias-chelate PA1 resin and magnetic sector inductively coupled plasma mass spectrometry (ICP-MS). *Mar. Chem.* **130–131**, 12–20. http://dx.doi.org/10.1016/j.marchem.2011.12.001.

Bishop (1988) The barite-opal carbon association in oceanic particulate matter. *Nature* **332**(341–343). http://dx.doi.org/10.1038/332341a0.

Boyle E. A. (1988) Cadmium: tracer of deepwater paleoceanography. *Paleoceanography* **3**(4), 471–489. http://dx.doi.org/10.1029/PA003i004p00471.

Boyle E. A., Sclater F. and Edmond J. M. (1976) On the marine geochemistry of cadmium. *Nature* **263**, 42–44. http://dx.doi.org/10.1038/263042a0.

Boyle E. A., John S. G., Abouchami W., Adkins J. F., Echegoyen-Sanz Y., Ellwood M., Flegal A. R., Fornace K., Gallon C., Galer S., Gault-Ringold M., Lacan F., Radic A., Rehkämper M., Rouxel O., Sohrin Y., Stirling C., Thompson C., Vance D., Xue Z. and Zhao Y. (2012) GEOTRACES IC1 (BATS) contamination-prone trace element isotopes Cd, Fe, Pb, Zn, Cu, and Mo intercalibration. *Limnol. Oceanogr.* **10**, 653–665. http://dx.doi.org/10.4319/lom.2012.10.653.

Bruland K. W. (1980) Oceanographic distributions of cadmium, zinc, nickel, and copper in the North Pacific. *Earth Planet. Sci. Lett.* **47**(2), 176–198. http://dx.doi.org/10.1016/0012-821x(80)90035-7.

Conway T. M. and John S. G. (2014a) Quantification of sources of dissolved iron to the North Atlantic Ocean. *Nature* **511**, 212–215. http://dx.doi.org/10.1038/nature13482.

Conway T. M. and John S. G. (2014b) The biogeochemical cycling of zinc and zinc isotopes in the North Atlantic Ocean. *Global Biogeochem. Cycles*. http://dx.doi.org/10.1002/2014GB004862.

Conway T. M., Rosenberg A. D., Adkins J. F. and John S. G. (2013) A new method for precise determination of iron, zinc and cadmium stable isotope ratios in seawater by double-spike mass spectrometry. *Anal. Chim. Acta* **793**, 44–52. http://dx.doi.org/10.1016/j.aca.2013.07.025.

Cutter G. A. and Bruland K. W. (2012) Rapid and noncontaminating sampling system for trace, elements in global ocean surveys. *Limnol. Oceanogr.* **10**, 425–436. http://dx.doi.org/10.4319/lom.2012.10.425.

de Souza G. F., Reynolds B. C., Rickli J., Frank M., Saito M. A., Gerringa L. J. A. and Bourdon B. (2012) Southern Ocean control of silicon stable isotope distribution in the deep Atlantic Ocean. *Global Biogeochem. Cycles* **26**. http://dx.doi.org/10.1029/2011GB004141.

Elderfield H. and Rickaby R. E. M. (2000) Oceanic Cd/P ratio and nutrient utilization in the glacial Southern Ocean. *Nature* **405**, 305–310. http://dx.doi.org/10.1038/35012507.

Gault-Ringold M., Adu T., Stirling C. H., Frew R. D. and Hunter K. A. (2012) Anomalous biogeochemical behavior of cadmium in subantarctic surface waters: mechanistic constraints from cadmium isotopes. *Earth Planet. Sci. Lett.* **341–343**, 94–103. http://dx.doi.org/10.1016/j.epsl.2012.06.005.

German C. R., Campbell A. C. and Edmond J. M. (1991) Hydrothermal scavenging at the Mid-Atlantic Ridge – modification of trace-element dissolved fluxes. *Earth Planet. Sci. Lett.* **107**(1), 101–114. http://dx.doi.org/10.1016/0012-821X(91)90047-L.

Ho T.-Y., You C.-F., Chou W.-C., Pai S.-C., Wen L.-S. and Sheu D. D. (2009) Cadmium and phosphorus cycling in the water column of the South China Sea: the roles of biotic and abiotic particles. *Mar. Chem.* **115**(1–2), 125–133. http://dx.doi.org/10.1016/j.marchem.2009.07.005.

Horner T. J., Lee R. B. Y., Henderson G. M. and Rickaby R. E. M. (2013) Nonspecific uptake and homeostasis drive the oceanic cadmium cycle. *Proc. Natl. Acad. Sci. USA* **110**(7), 2500–2505. http://dx.doi.org/10.1073/pnas.1213857110.

Janssen D. J., Conway T. M., John S. G., Christian J., Kramer D. I., Pederson T. F. and Cullen J. T. (2014) An undocumented water column sink for cadmium in open ocean oxygen deficient zones. *Proc. Natl. Acad. Sci. USA* **111**(19), 6888–6893. http://dx.doi.org/10.1073/pnas.1402388111.

Jenkins W. I., Smethie W. M, Boyle E. A. and Cutter G. C. (2014) Water mass analysis for the U.S. GEOTRACES North Atlantic sections. *Deep Sea Res. Part II* (in press).

John S. G. (2012) Optimizing sample and spike concentrations for isotopic analysis by double-spike ICPMS. *J. Anal. At. Spectrom.* **27**, 2123–2131. http://dx.doi.org/10.1039/c2ja30215b.

John S. G. and Adkins J. (2012) The vertical distribution of iron stable isotopes in the North Atlantic near Bermuda. *Global Biogeochem. Cycles* **26**(2). http://dx.doi.org/10.1029/2011GB004043.

John S. G. and Conway T. M. (2014) A role for scavenging in the marine biogeochemical cycling of zinc and zinc isotopes. *Earth Planet. Sci. Lett.* **394**, 159–167. http://dx.doi.org/10.1016/j.epsl.2014.02.053.

Klevenz V., Bach W., Schmidt K., Hentscher M., Koschinsky A. and Petersen S. (2011) Geochemistry of vent fluid particles formed during initial hydrothermal fluid–seawater mixing along the Mid-Atlantic Ridge. *Geochem. Geophys. Geosyst.* **12**(10). http://dx.doi.org/10.1029/2011GC003704.

Lacan F., Francois R., Ji Y. C. and Sherrell R. M. (2006) Cadmium isotopic composition in the ocean. *Geochim. Cosmochim. Acta* **70**(20), 5104–5118. http://dx.doi.org/10.1016/j.gca.2006.07.036.

Lambelet M., Rehkämper M., Van de Flierdt T., Xue Z., Kreissig K., Coles B., Porcelli D. and Andersson P. (2013) Isotopic analysis of Cd in the mixing zone of Siberian rivers with the Arctic Ocean—new constraints on marine Cd cycling and the isotope composition of riverine Cd. *Earth Planet. Sci. Lett.* **361**, 64–73. http://dx.doi.org/10.1016/j.epsl.2012.11.034.

Lane T. W. and Morel F. M. M. (2000) A biological function for cadmium in marine diatoms. *Proc. Natl. Acad. Sci. USA* **97**(9), 4627–4631. http://dx.doi.org/10.1073/pnas.090091397.

Lane T. W., Saito M. A., George G. N., Pickering I. J., Prince R. C. and Morel F. M. M. (2005) A cadmium enzyme from a marine diatom. *Nature* **435**, 42. http://dx.doi.org/10.1038/435042a.

Ohnemus D. C. and Lam P. J. (2014) Cycling of lithogenic marine particulates in the US GEOTRACES North Atlantic transect. *Deep Sea Res. Part II* (in press).

Palter J. B., Lozier M. S. and Barber R. T. (2005) The effect of advection on the nutrient reservoir in the North Atlantic subtropical gyre. *Nature* **437**, 687–692. http://dx.doi.org/10.1038/nature03969.

Price N. M. and Morel F. M. M. (1990) Cadmium and cobalt substitution for zinc in a marine diatom. *Nature* **344**, 658–660. http://dx.doi.org/10.1038/344658a0.

Rehkämper M., Wombacher F., Horner T. J. and Xue Z. (2012) Natural and anthropogenic Cd isotope variations. In: *Handbook of Environmental Isotope Geochemistry Advances in Isotope*

Geochemistry. pp. 125–154. http://dx.doi.org/10.1007/978-3-642-10637-8_8.

Revels B. N. (2013) Chemical leaching methods for measurements of marine labile particulate [Fe] and δ^{56}Fe. M. S. thesis, Univ. South Carolina.

Ripperger S. and Rehkämper M. (2007) Precise determination of cadmium isotope fractionation in seawater by double spike MC-ICPMS. *Geochim. Cosmochim. Acta* **71**(3), 631–642. http://dx.doi.org/10.1016/j.gca.2006.10.005.

Ripperger S., Rehkämper M., Porcelli D. and Halliday A. N. (2007) Cadmium isotope fractionation in seawater – a signature of biological activity. *Earth Planet. Sci. Lett.* **261**(3–4), 670–684. http://dx.doi.org/10.1016/j.epsl.2007.07.034.

Rosenthal Y., Boyle E. A., Labeyrie L. and Oppo D. (1995) Glacial enrichments of authigenic Cd and U in subantarctic sediments: a climatic control on the elements' oceanic budget? *Paleoceanography* **10**(3), 395–413. http://dx.doi.org/10.1029/95PA00310.

Saito M. A., Noble A. E., Goepfert T. J., Lamborg C. H. and Jenkins W. J. (2013) Slow-spreading submarine ridges in the South Atlantic as a significant iron source. *Nat. Geosci.* **6**, 775–779. http://dx.doi.org/10.1038/ngeo1893.

Schlitzer R. (2014) eGEOTRACES – Electronic Atlas of GEOTRACES Sections and Animated 3D Scenes. http://www.egeotraces.org.

Schmitt A.-D., Galer S. J. G. and Abouchami W. (2009) Mass-dependent cadmium isotopic variations in nature with emphasis on the marine environment. *Earth Planet. Sci. Lett.* **277**(1–2), 262–272. http://dx.doi.org/10.1016/j.epsl.2008.10.025.

Siebert C., Nagler T. F. and Kramers J. D. (2001) Determination of molybdenum isotope fractionation by double-spike multicollector inductively coupled plasma mass spectrometry. *Geochem. Geophys. Geosyst.* **2**(7). http://dx.doi.org/10.1029/2000GC000124.

Sunda W. G. and Huntsman S. A. (1996) Antagonisms between cadmium and zinc toxicity and manganese limitation in a coastal diatom. *Limnol. Oceanogr.* **41**(3), 373–387.

Taylor S. R. (1964) Abundance of chemical elements in the continental crust: a new table. *Geochim. Cosmochim. Acta* **28**, 1273–1285. http://dx.doi.org/10.1016/0016-7037(64)90129-2.

Van Geen A., McCorkle D. C. and Klinkhammer G. P. (1995) Sensitivity of the phosphate–cadmium–carbon isotope relation in the ocean to cadmium removal by sub-oxic sediments. *Paleoceanography* **10**(2), 159–169. http://dx.doi.org/10.1029/94PA03352.

Wright J. J., Konwar K. M. and Hallam S. J. (2012) Microbial ecology of expanding oxygen minimum zones. *Nat. Rev. Microbiol.* **10**(6), 381–394. http://dx.doi.org/10.1038/nrmicro2778.

Xue Z. C., Rehkämper M., Schonbachler M., Statham P. J. and Coles B. J. (2012) A new methodology for precise cadmium isotope analyses of seawater. *Anal. Bioanal. Chem.* **402**(2), 883–893. http://dx.doi.org/10.1007/s00216-011-5487-0.

Xue Z., Rehkämper M., Horner T. J., Abouchami W., Middag R., Van de Flierd T. and De Baar H. J. W. (2013) Cadmium isotope variations in the Southern Ocean. *Earth Planet. Sci. Lett.* **382**, 161–172. http://dx.doi.org/10.1016/j.epsl.2013.09.014.

Yang S.-C., Lee D.-C. and Ho T.-Y. (2012) The isotopic composition of cadmium in the water column of the South China Sea. *Geochim. Cosmochim. Acta* **98**, 66–77. http://dx.doi.org/10.1016/j.gca.2012.09.022.

Associate editor: Claudine Stirling